

Performance and Evaluation of Multisensor Precipitation Estimation Algorithm Using a High Density Rain Gauge Network and Hydrologic Simulation

ALEJANDRA M. ROJAS GONZÁLEZ¹, ERIC W. HARMSSEN², SANDRA CRUZ POL³

¹Department of Civil Engineering
University of Puerto Rico – Mayagüez Campus
Mayagüez, PR 00680. U.S.A.
alejandra.rojas@upr.edu

²Department of Agricultural and Biosystems Engineering
University of Puerto Rico – Mayagüez Campus
P.O. Box 9030, Mayagüez, PR 00681, U.S.A.
eric.harmsen@upr.edu <http://academic.uprm.edu/abe/PRAGWATER>

³Department of Computer and Electrical Engineering
University of Puerto Rico – Mayagüez Campus
P.O. Box 9030, Mayagüez, PR 00681, U.S.A.
sandracruzpol@ieee.org

Abstract: A rain gauge network (28 rain gauges) was installed in western Puerto Rico (PR) within a 4km x 4km GOES satellite pixel. Located within the pixel is a well monitored sub-watershed of 3.55 km², referred to here as the “testbed subwatershed” (TBSW). The rain gauge network was established to evaluate the performance of the GOES-based Hydro-Estimator (HE) rain rate algorithm, and estimated rain rates from NEXRAD radar and the Center for Collaborative Adaptive Sensing of the Atmosphere (CASA) radar network, which has a high spatial resolution (approximated 200 m). Furthermore, the rain gauge network will provide a high temporal and spatial resolution rainfall dataset to be input into a distributed hydrologic model in the TBSW. The focus of this work is to evaluate the performance of the Multisensor Precipitation Estimation (MPE) product at 1hour and 1day temporal resolution within the 4km x 4km HE pixel and at watershed level for 2007. The MPE product is popular within the hydrologic modeling community due to its resolution and mean field bias correction computations in its coverage. Results for 2007 indicate that the highest rainfall measured by the rain gauges within the HE pixel area were September with an average and standard deviation of 241.75 mm and 73.3 mm, respectively; and August with 223.7 mm and 64.66 mm, respectively. While for the same months the Multisensor Precipitation Estimation, produced a total monthly rainfall accumulation and standard deviation of 247.36 mm and 64.4 mm for September, respectively, and 233.68 mm and 36.54 mm for August, respectively. The mean and standard deviation daily field bias for these months were 1.08 and 1.5 for September, respectively, and 0.93 and 1.6 for August, respectively. The bias changed, when considering an hourly analysis, to 1.98 average and 5.45 standard deviation for August and 1.49 average and 3.01 standard deviation for September.

Keywords: Multisensor Precipitation Estimation, NEXRAD products, rainfall variability, mean field bias, hydrology, distributed model.

Introduction

In western Puerto Rico a study is being conducted to develop a Doppler and polarimetric radar network operating with a frequency of 9.8 gigahertz (X band). This radar network will provide an effective way to

predict the weather conditions in western Puerto Rico at a high spatial resolution, and will provide precipitation estimates for flood forecasting models. A major source of error in hydrologic models is the poor quantification of the areal distribution of rainfall, typically due to the low density of rain gauges. A rain gauge located at a single point may represent an extensive area, typically greater than 107 m², with only one value, which much of the time does not representative the average rainfall, especially in areas of high topographic variability subject to convection storms (Wilson et al., 1979). Rain gauges themselves may produce errors, a major source of error being from turbulence and increased winds around the gauge, affecting precipitation quantification in events where the wind is an important factor (e.g., hurricanes). Investigators have used mean areal precipitation as calculated by, for example Thiessen polygons, (Wilson et al., 1979 and Viessman et al., 1996), and interpolation methods, such as spline, inverse distance weighted, and krigging. But all these methods are limited by the numbers of rain gauges and how they represent the spatial rainfall distribution. Currently, sophisticated methods attempt to fill gaps between rain gauges, by sensing the atmosphere with remote sensors like the spaceborne Tropical Rainfall Measuring Mission (TRMM); the National Oceanic and Atmospheric Administration's (NOAA) Hydro Estimator (HE) algorithm (Scofield et al., 2003); the National Weather Service's (NWS) Next Generation Radar (NEXRAD), and the Multisensor Precipitation Estimation Algorithm (MPE). The HE utilizes data from the GOES geostationary satellite to estimate rainfall, and has, for example, an approximate pixel size of 4 km. NEXRAD estimates rainfall within a radial coordinate system with a base resolution of 2 to 4 km. These quantitative precipitation estimation (QPE) techniques are evaluated and adjusted or calibrated using existing rain gauges, however, these adjustments depend on the rain gauge density and their spatial distribution.

Studies that have compared radar and rain gauge-derived rainfall have documented large discrepancies between the two, e.g. Scofield and Kuligowski (2003), Baeck and Smith (1998) and McGregor et al. (1995). The MPE algorithm is a product of NEXRAD, and has recently replaced the Stage II and III algorithms. MPE is based on multiyear climatology of the Digital Precipitation Array (DPA) product (temporal resolution is 1 hour, spatial resolution is 4 km) and performs a mean field bias correction over the entire radar coverage area, based on (near) real time hourly rain gauge data (Seo et al., 1999). The MPE is mapped onto a polar stereographic projection called the Hydrologic Rainfall Analysis Project (HRAP) grid.

With the objective to calibrate and validate the high density CASA radar network in western PR, a rain gauge network (28 tipping buckets rain gauges) was installed in a small highland area. The rain gauge network is located within a single GOES HE pixel (4 km) and 18 of the 28 rain gauges are within in a testbed subwatershed (TBSW). The rain gauge network will provide a high resolution rainfall data set to evaluate the CASA radars, calculate the NEXRAD products and Hydro Estimator uncertainty under their typical resolution (Harmsen et al., 2008), and understand the hydrologic response and predictability limits due to rainfall and topographic resolution using a distributed hydrologic model to capture the spatial variations. The TBSW has an area of 3.55 km², belongs to Río Grande de Añasco watershed, has an average 29% slope, the predominant soil hydrologic group is C, and the surface soil has an average 3.25 cm/hr hydraulic conductivity.

Methodology

In this study we evaluated the performance of the MPE product within the HE pixel for 2007 using the rain gauge network. In 2006, sixteen tipping bucket rain gauges (Spectrum Technology, Inc.2) were installed uniformly within the Hydro-Estimator (HE) pixel (Harmsen et al., 2008). From June 2007 another 12 tipping bucket rain gauges were added to the network located within the TBSW. For this study we analyzed the 28 rain gauges for the 2007 year and compared the gauge data with the MPE algorithm.

The maximum, average and standard deviation distance between the 28 rain gauges were calculated using Euclidian Distance are 829 m, 334 m and 171 m, respectively. These statistical parameters were reduced within TBSW as follows: 563 m, 218 m and 100 m, respectively. Figure 1, shows the rain gauge network, the TBSW outline and the distance between rain gauges. Some stations were not operating during some periods, owing to gauge damage or low data logger batteries, these data were eliminated from the analysis. Five minute data were accumulated to 1 hour and daily accumulations, with the intention of comparing the rain gauge data with the MPE pixels.

MPE pixels are based on a HRAP grid. Therefore, a geographic coordinate transformation from Stereographic North Pole to NAD 1983 State Plane Puerto Rico and Virgin Islands was performed for each hour using the ArcGIS project raster tool.

The re-sampling technique algorithm used was the nearest neighbor assignment at 4 km resolution. Due to changes in coordinates and raster conversions, the original pixels are oriented horizontally. Figure 2 displays the change in the orientation, including the MPE pixels (left) and Hourly Rainfall Product (N1P) from NEXRAD level 3 (right). The left image shows four square black boxes corresponding to the MPE

raster projected pixels and the colored pixels are the original raster with HRAP coordinates. In the right image, the black boxes are from the shapefile and the colored pixels are raster projected data.

The NIP rainfall product is calculated from NEXRAD as a rain rate each 5 or 6 minutes when the radar detects rainfall, and a 10 minute NIP product is archived when no rainfall is detected.

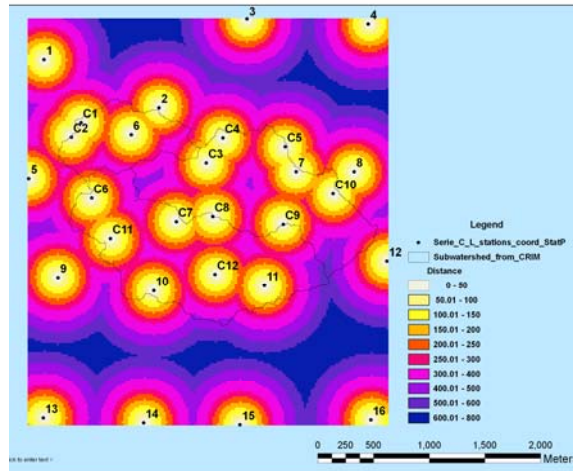


Figure 1. Rain gauge distribution and location within a HE pixel, Tesbed SubWatershed location and Euclidean Distance between the stations.

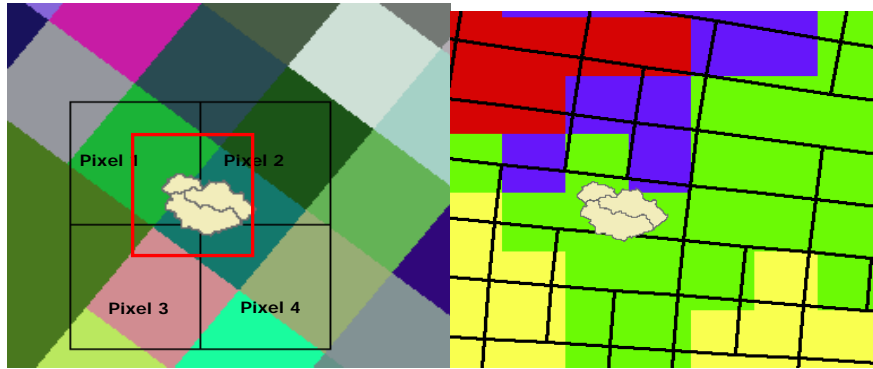


Figure 2. MPE pixels (left) at different geographic coordinates and the HE pixel at 4 km resolution (red box). Hourly rainfall product from NEXRAD level 3 (right) as shapefile and raster format. The TBSW is also shown near the center of the four MPE pixels.

The original geographic coordinate system (GCS) is polar, and using the NOAA Weather and Climate Toolkit Exporter it is possible to transform the coordinates to GCS_WGS_1984. Different formats are available to export the data. The shape files maintain the original orientation; however, in a distributed hydrologic model it is necessary to use raster or ASCII files to represent the spatial rainfall variation in the model. Due to raster characteristics it is not possible to maintain the original orientation. Figure 2, right image, shows the shapefile in black lines and a rainfall raster as colored pixels, both at 2 km resolution.

The study was made with the projection pixels because these will be the input to the distributed hydrologic model. With the aforementioned in mind, 4 MPE pixels were obtained around the HE pixel, identified as Pixel 1 (top left), Pixel 2, Pixel 3 and Pixel 4 (bottom right), Figure 2 (left). Area weights were calculated for intersecting areas between the MPE pixels and the HE pixel and are 0.281, 0.344, 0.169 and 0.206, respectively. These area weights are used to calculate the mean field bias with the rain gauges, obtain an average map precipitation for each time step, and to calculate the percentage of detection and false alarms evaluated with contingency tables, where the rain gauges are the “ground truth” values and the MPE

are the estimated values. In this way can be evaluated the accuracy of the rainfall detection in terms of hit rate “H”, probability of detection “POD”, false-alarm rate “FAR” and discrete bias “DB” (Ramírez-Beltrán et al., 2008) Weights for the N1P radar product were also estimated for 9 partial pixels within the HE pixel (Figure 2, left). The indicators to evaluate the accuracy of MPE rainfall estimations over the HE pixel at different temporal scales are the root mean square error (RMSE) and normalized bias (NBIAS).

To illustrate the variability of the rainfall distribution within a specific pixel, we considered the MPE Pixels 1 and 2 and identified the rain gauge stations associated them. For MPE Pixel 1, the associated rain gauges are: C01, C02, C03, C06, C07 C11, L01, L02, L05, L06 and L09, and for MPE Pixel 2 the associated rain gauges are: C04, C05, C08, C09, C10, C12, L03, L04, L07, L08, L10, L11. A mean field bias was calculated for the 1 hour time resolution. The gauges L06 and L08 showed systematic errors in the records and, therefore, were ignored in the calculations. In addition to the statistics computed in the MPE Pixels 1 and 2, calculations were made using the 4 MPE pixels and the 26 rain gauges for hourly and daily data.

Results and Discussion

The annual 2007 rainfall for the 4 MPE pixels were 1546.2, 2212.1, 1949.8 and 2088.6 mm, with an annual standard deviation of 289.3 mm. Figure 3 shows the temporal variations in the cumulative rainfall during the year for each MPE Pixel. To show how variable the rainfall distribution within a specific pixel can be, we took the MPE Pixels numbers 1 and 2 and determined the rain gauges associated with each pixel. A plot of the monthly cumulative rainfall for MPE Pixel 1 and the rain gauges is displayed in Figure 4. The cumulative rainfall for the months of April and May are not representative of those months because we had missing rain gauge data for 11 days for April and 9 days for May, therefore, the computations were made with only the available data for these months. For the case of July, Figure 4 shows that only the C06 station reported an amount of rainfall (206.9 mm) that was similar to the MPE Pixel 1 rainfall (259.15 mm), and for almost all months, note that the MPE Pixel 1 underestimated rainfall, except for the months of January, June and July.

A mean field bias was calculated for the MPE Pixel 1 and 2 by averaging the rain gauge rainfall and dividing by the rainfall sensed for the MPE pixel for each time step (1 hour). A time series bias was calculated for MPE Pixel 1 (Figure 5) and MPE Pixel 2 (Figure 6).

Furthermore, this calculation was made for all stations and the four pixels (Figure 7). The bias tended to decrease when the calculation was performed for the whole HE pixel area (16 km²). Large bias computations were found at the hourly time step and are associated with small rainfall radar detections.

Because, the minimum precipitation depth that the radar is capable of detecting is 0.01 inches or 0.00394 mm; while our rain gauge network has a rainfall depth resolution of 0.1 mm. Therefore when the MPE is accumulated (e.g., over several hours or days) the bias is reduced and the standard deviation as well. Table 1 provides detailed bias computations for 2007.

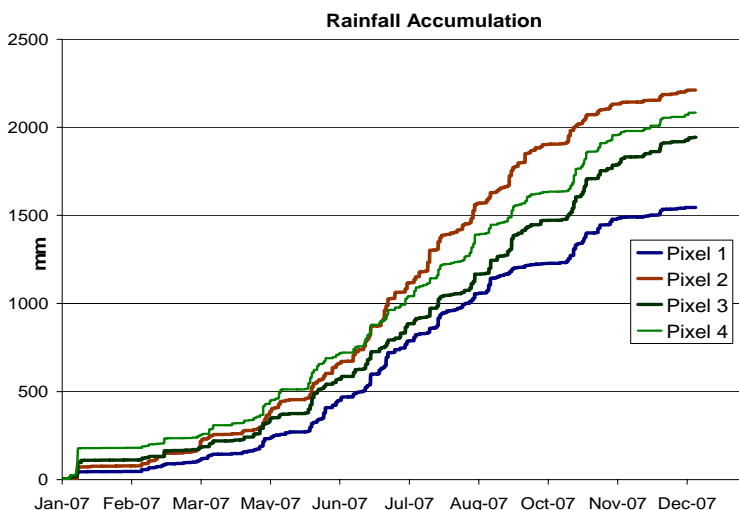


Figure 3. Rainfall accumulation over the time for the MPE pixels.

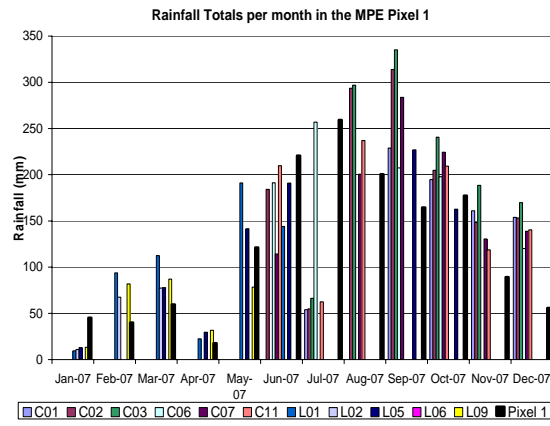


Figure 4. Monthly Total Rainfall calculation for the rain gauge stations belongs to MPE Pixel 1, for 2007.

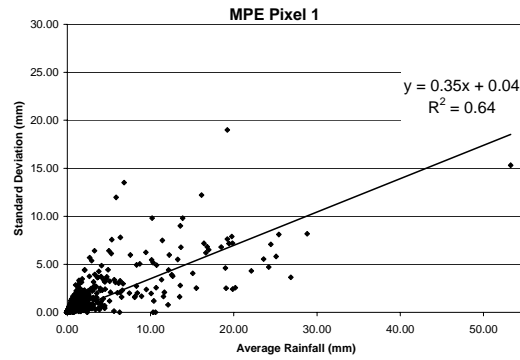


Figure 5. Hourly average and standard deviation rainfall for the rain gauges corresponding to MPE pixel 1 for the 2007.

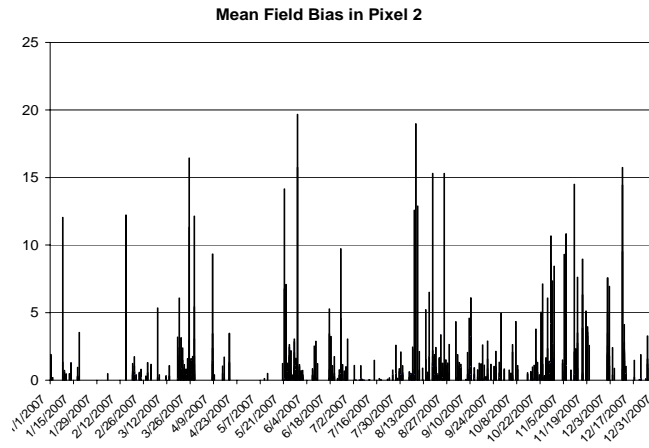


Figure 6. Hourly Mean Field Bias for the MPE Pixel 2 for 2007 year within a HE Pixel.

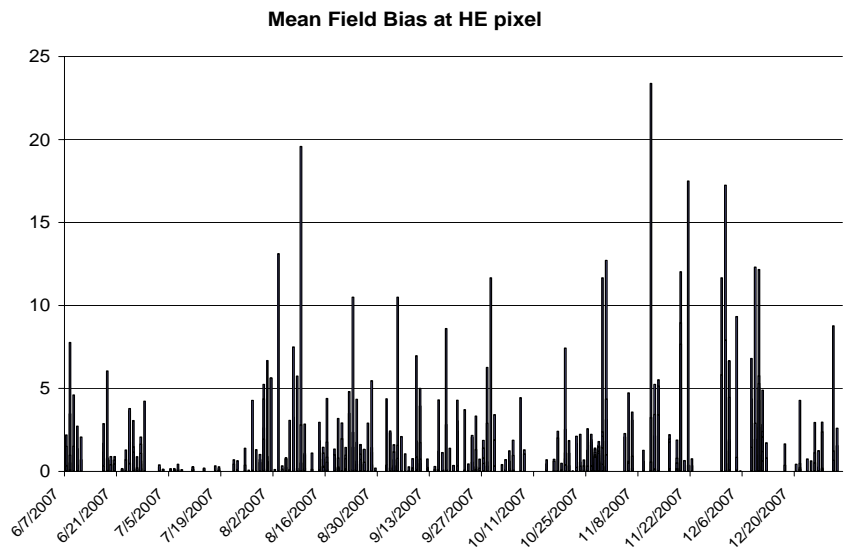


Figure 7. Hourly Mean Field Bias for the MPE Pixels within a HE Pixel for June to December 2007.

Figures 8 and 9, show the number of false alarms by the radar. Events in which the radar did not detect rainfall and the rain gauges did measure rainfall were assigned a value of 1 in the graph. Events in which the radar did detect rainfall and the gauges did not measure rainfall were assigned a value of 2. Differences in times when false alarms occurred can be observed in the graphs, and detailed statistics are presented in Table 1 and 2. The biases were calculated in hourly and daily time steps. An average for 2007 period from hourly data is shown in Table 1. Table 2 provides the results for the hourly bias calculation to demonstrate the monthly trends. The results indicate that the month with largest daily bias was November (2.24), which also had the highest variability.

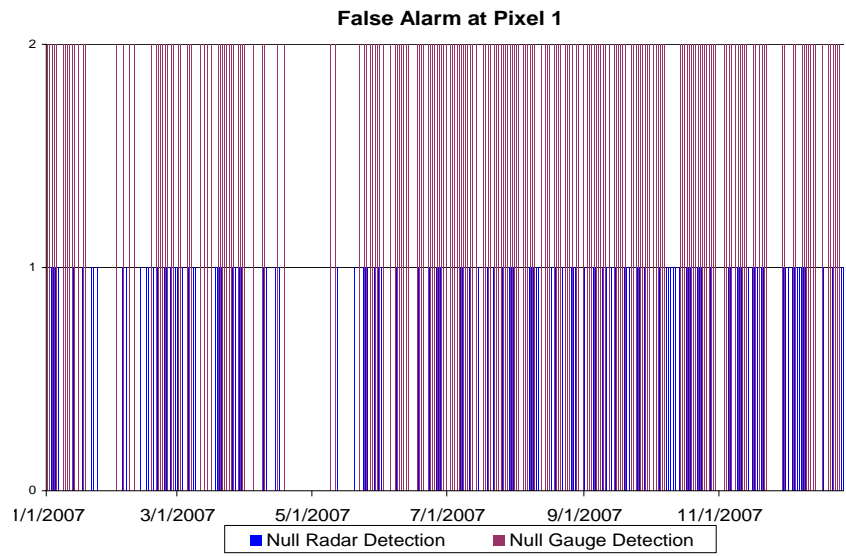


Figure 8. Hourly False Alarm Time Series for the MPE Pixel 1 for 2007.

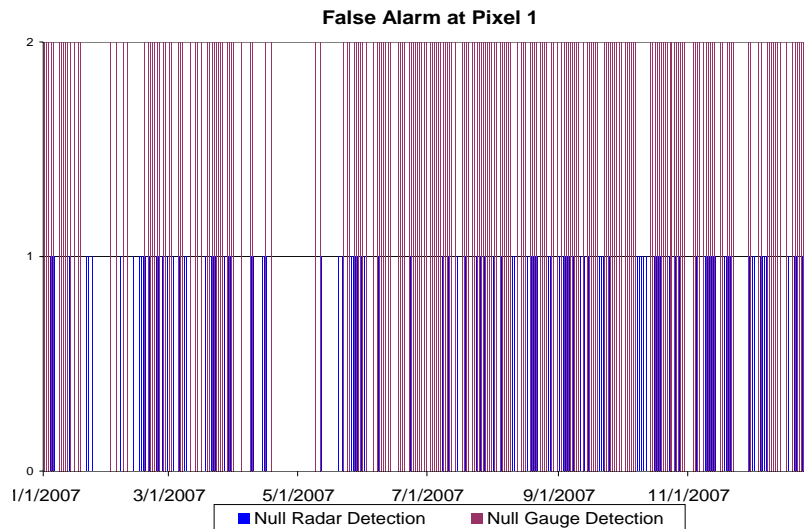


Figure 9. Hourly False Alarm Time Series for the MPE Pixels within a HE Pixel for June to December 2007

Table 1. Discrete validation scores for the Pixel 1, Pixel 2 and 4 MPE Pixels and time scales.

	Hourly Data			Daily Data
	MPE Pixel 1	MPE Pixel 2	4 MPE pixels	4 MPE pixels
POD	0.62	0.58	0.57	0.833
FAR	0.51	0.42	0.45	0.128
DB	1.24	1.01	1.04	0.956
H	0.87	0.89	0.82	0.879

Table 2. Total rainfall in the MPE pixels and mean field daily bias calculation.

	MPE Statistics		Rain Gauge	Month Bias	Day Bias		Hour Bias		Hour Bias Rain>0.3mm	
	Mean	STD	Total	Mean	Mean	STD	Mean	STD	Mean	STD
Jan	94.9	57.3	15.5	0.16	1.43	1.81	2.47	4.77	0.60	2.02
Feb	56.5	13.4	71.5	1.27	1.20	1.91	2.89	9.11	2.57	2.80
Mar	78.4	23.0	94.6	1.21	1.36	1.38	1.48	1.89	2.18	1.98
Apr	120.9	21.3								
May	187.0	34.5								
Jun	235.0	39.2	192	0.82	1.02	0.85	3.25	10.59	1.26	1.44
Jul	316.6	87.4	82.2	0.26	0.97	1.51	1.04	2.68	0.39	0.88
Aug	233.7	36.5	223.7	0.96	0.93	1.60	1.98	5.45	1.66	2.44
Sept	247.4	64.4	241.5	0.98	1.08	1.50	1.49	3.01	1.61	1.58
Oct	208.0	40.6	204.2	0.98	0.72	0.50	1.14	1.74	1.19	0.99
Nov	95.1	24.4	162.5	1.71	2.24	2.60	3.92	8.16	2.92	4.55
Dec	79.4	27.2	109.9	1.38	1.72	2.38	5.68	12.92	1.53	2.52
Year	1952.7	249.8	1542.3	0.85	1.24	1.65	2.77	8.14	1.55	2.14

Conclusion

Multisensor Precipitation Estimation algorithm is developed by National Weather Service to improve the NEXRAD rainfall quantifications applying an hourly bias correction over the radar coverage. In western Puerto Rico the raingauge density to correct the MPE algorithm is poor and the bias calculated could not apply to this region or small watersheds, incorporating an error in the hydrologic simulation. The MPE algorithm is evaluated at small scale into the Hydro-Estimator pixel where match 4 MPE pixels. Individual and overall MPE pixels were evaluated at different time scales.

The MPE performance at major time scales (daily) generally was better, except for the months of January, July, November and December comparing them with the monthly mean field bias. The hourly Bias computation presented in the Table 4 for the months could be enhanced suppressing light rainfall less than 0.3 mm in the radar and raingauge averages, except for the months of March and September. For January and July was archived a big bias reduction (0.6 and 0.39 respectively) comparable with the monthly bias computations (0.16 and 0.26). Exist important monthly Bias variations in the average MPE pixels compared to the ratio of average raingauge network and total annual MPE rainfall at 4 pixels (0.85).

In a future study should extend the area to cover not only the TBSW else the raingauges that are into the Río Grande de Añasco and Guanajibo basins to validate the MPE algorithm and correct the rainfall quantification by a new bias factor in the hydrologic modeling.

NEXRAD Level 3 (N1P) quantification will be performed and compared with the rain gauge network data, generating surfaces at each time step within the HE pixel and the TBSW. It is imperative to measure the performance of the QPE at scales below the 2km x 2km (N1P) resolution and quantify how the hydrologic response is affected by temporal and spatial precipitations resolutions.

Acknowledgements. This material is based on research supported by NOAA-CREST (NA17AE1625), NSF-CASA, NASA-IDEAS and USDA Hatch (H-402).

References

- Baeck, M. L., and J. A. Smith, 1998. Estimation of heavy rainfall by the WSR-88D. *Weather Forecasting*, 13, 416–436.
- Casale, R. and C. Margottini, 2004. Natural Disasters and Sustainable Development. Springer, 41 pp.
- Harmsen, E.W., S.E. Gomez-Mesa, E. Cabassa, N.D. Ramirez-Beltrán, S. Cruz-Pol, R.J. Kuligowski and R. Vásquez, 2008. Satellite Sub-Pixel Rainfall Variability. *International J of Sys. Appl., Eng. & Devel.*, Volume 2, Issue 3, pp 91-100.
- McGregor, K. C., R. L. Bingner, A. J. Bowie, and G. R. Foster, 1995. Erosivity index values for northern Mississippi. *Trans. ASCE*, 38, 1039–1047.
- Ramirez-Beltrán, N.D., R.J. Kuligowski, E.W. Harmsen, J.M. Castro, S. Cruz-Pol and M.J. Cardona-Soto, 2008. Validation and Strategies to Improve the Hydro-Estimator and NEXRAD over Puerto Rico. 12th WSEAS International Conference on SYSTEMS, Heraklion, Greece, July 22-24, 2008.
- Scofield, R.A. and R.J. Kuligowski, 2003. Status and outlook of operational satellite precipitation algorithms for extreme-precipitation events. *Weather and Forecasting*, 18(6): 1037-1051.
- Seo, D.J, J. P. Briedenbach, and E. R. Johnson, 1999. Real-time estimation of mean field bias in radar rainfall data. *J. Hydrol.*, 223(3-4): 131–147.
- Stellman, K.M., H.E. Fuelberg., R. Garza, M. Mullusky, 2001: An Examination of Radar and Rain Gauge–Derived Mean Areal Precipitation over Georgia Watersheds. *American Meteorological Society Journal*. Volume 16, Issue 1, February 2001.
- Vieux, B.E., 2004. Distributed Hydrologic Modeling using GIS. Second Edition. Kluwer Academic, The Netherlands, 164 pp.
- Viessman, W., and G. L. Lewis, 1996: Introduction to Hydrology. 4th Edition, Harper-Collins, 760 pp.
- Wilson, J. W. and E. A. Brandes, 1979: Radar measurement of rainfall –A summary. *Bulletin of the AMS*, Vo.l. 60., Issue 9, Sept., pp 1048-1058.
- Woodley, W. L., A. R. Olsen, A. Herndon, and V. Wiggert, 1975: Comparison of gauge and radar methods of convective rain measurement. *J. Appl. Meteor.*, 14, 909–928.
- Wilks, D.S., 1995: Statistical Methods in the Atmospheric Sciences: An Introduction. Academic Press, San Diego, 467 pp.